

On the Origin of the Monoclinic Distortion in Li_xNiO_2

M. E. Arroyo y de Dompablo* and G. Ceder

Department of Material Science and Engineering, Massachusetts Institute of Technology,
Cambridge, Massachusetts 02139

Received March 19, 2002. Revised Manuscript Received September 4, 2002

Using first-principles calculation and thermally equilibrated Li-vacancy configurations, we have calculated the monoclinicity, a_m/b_m , as a function of lithium content in Li_xNiO_2 . In agreement with experimental data, maxima in a_m/b_m are predicted around $\text{Li}_{0.75}\text{NiO}_2$ and $\text{Li}_{0.4}\text{NiO}_2$. We explain the monoclinicity maxima at $\text{Li}_{0.75}\text{NiO}_2$ in terms of a Jahn–Teller distortion assisted by the presence of lithium-vacancy ordering. The subsequent removal of lithium causes a decrease in the number of Ni^{3+} ions and therefore in the monoclinicity. However, the strong lithium-vacancy ordering at $\text{Li}_{0.4}\text{NiO}_2$ enables new maxima of monoclinicity despite the low Ni^{3+} content.

Introduction

LiNiO_2 has been the focus of significant attention due to its high energy density and capacity in lithium battery applications.¹ Layered LiMO_2 compounds ($M = \text{Co}, \text{Ni}, \text{Mn}$, etc.) can be viewed as “ordered rock salts” in which alternate layers of Li^+ and M^{+3} ions occur in octahedral sites within the ccp oxygen array, making up a rhombohedral structure.² In LiNiO_2 Ni^{3+} is in a low spin state $(t_{2g})^6(e_g)^1$, so the degeneracy of the two e_g levels gives the Ni^{3+} potential Jahn–Teller activity. Indeed, EXAFS studies have shown that in this compound the Ni^{3+} –O octahedra are locally Jahn–Teller-distorted.^{3,4} However, unlike LiMnO_2 , where the long-range order of the local J–T distortions leads to a reduction of the unit cell symmetry from $R\bar{3}m$ to $C2/m$,⁵ such a cooperative distortion has never been observed in LiNiO_2 ,^{1,3,4,6,7} even though it has been predicted to be stable by first-principles calculations.⁸ This discrepancy is likely due to the departure from stoichiometry in the experimental LiNiO_2 compounds, whereby excess of Ni occupy Li sites ($\text{Li}_{1-z}\text{Ni}_{1+z}\text{O}_2$).³

Electrochemical and chemical removal of lithium in Li_xNiO_2 leads to a reduction in symmetry from rhombohedral to monoclinic. This monoclinic region occurs for $0.4 < x < 0.75$.^{1,7,9–13} The material shows excellent

electrochemical performance in this phase domain,^{1,7,14} which spans most of the useful range for use of Li_xNiO_2 as an electrode in lithium batteries. For $x < 0.4$ the material regains rhombohedral symmetry.¹⁰ The origin of the large monoclinic region is controversial. One possible and obvious driving force is a cooperative distortion of NiO_2 octahedra^{12,15,16} due to the Jahn–Teller (J–T) effect of trivalent nickel ions. However, as has been claimed by some authors,^{1,7,14} this cause of the monoclinicity is somewhat unlikely: since a cooperative J–T distortion is not present in LiNiO_2 , it is unlikely that a material with a lower concentration of J–T-distorted Ni^{3+} octahedra can have a collective J–T distortion. Since lithium removal also creates vacancies, Li-vacancy ordering can take place. Hence, it has been speculated that such Li ordering may be the cause of the monoclinic distortion in partially delithiated Li_xNiO_2 .^{14,17} The fact that a monoclinic ordered phase has been well-characterized in $\text{Li}_{0.5}\text{CoO}_2$, both with theoretical¹⁸ and experimental methods,¹⁹ gives credibility to the Li-vacancy ordering argument. There are however significant differences between Li_xNiO_2 and Li_xCoO_2 . In Li_xCoO_2 the monoclinic phase region is narrower in composition and centered around $x = 0.5$, whereas in Li_xNiO_2 it is found from $x = 0.4$ to $x = 0.75$. Furthermore, the monoclinic distortion in Li_xNiO_2 ($a_m/b_m =$

(1) Delmas, C.; Menetrier, M.; Croguennec, L.; Levasseur, S.; Peres, J. P.; Pouillere, C.; Prado, G.; Fournes, L.; Weill, F. *Int. J. Inorg. Mater.* **1999**, *1*, 11.

(2) Goodenough, J. B.; Wickham, D. G.; Croft, W. J. *J. Phys. Chem. Solids* **1958**, *5*, 107.

(3) Rougier, A.; Delmas, C.; Chadwick, A. V. *Solid State Commun.* **1995**, *94*, 123.

(4) Mansour, A. N.; Yang, X. Q.; Sun, X.; McBreen, J.; Croguennec, L.; Delmas, C. *J. Electrochem. Soc.* **2000**, *147*, 2104.

(5) Armstrong, A. R.; Bruce, P. G. *Nature* **1996**, *381*, 499.

(6) Thomas, M. G. S. R.; David, W. I. F.; Goodenough, J. B.; Groves, P. *Mater. Res. Bull.* **1985**, *20*, 137.

(7) Peres, J. P.; Demourgues, A.; Delmas, C. *Solid State Ionics* **1998**, *111*, 135.

(8) Marianetti, C.; Morgan, D.; Ceder, G. *Phys. Rev. B* **2001**, *63*, 224304.

(9) Arai, H.; Okada, S.; Sakurai, Y.; Yamaki, J. *Solid State Ionics* **1997**, *95*, 275.

(10) Croguennec, L.; Pouillere, C.; Delmas, C. *J. Electrochem. Soc.* **2000**, *147* (4), 1314.

(11) Hirano, A.; Kanno, R.; Kawamoto, Y.; Takeda, Y.; Yamaura, K.; Takano, M.; Ohyama, K.; Ohashi, M.; Yamaguchi, Y. *Solid State Ionics* **1995**, *78*, 123.

(12) Ohzuku, T.; Ueda, A.; Nagayama, M. *J. Electrochem. Soc.* **1993**, *140*, 1862.

(13) Li, W.; Reimers, J. N.; Dahn, J. R. *Solid State Ionics* **1993**, *67*, 123.

(14) Delmas, C.; Peres, J. P.; Rougier, A.; Demourgues, A.; Weill, F.; Chadwick, A.; Broussely, M.; Perton, F.; Biensan, Ph.; Willmann, P. *J. Power Sources* **1997**, *68*, 120.

(15) Hirano, A.; Kanno, R.; Kawamoto, Y.; Oikawa, K.; Kamiyama, T.; Izumi, F. *Solid State Ionics* **1996**, *86–88*, 791.

(16) Arai, H.; Okada, S.; Ohtsuka, H.; Ichimura, M.; Yamaki, J. *Solid State Ionics* **1995**, *80*, 261.

(17) Peres, J. P.; Weill, F.; Delmas, C. *Solid State Ionics* **1999**, *116*, 19.

(18) Van der Ven, A.; Aydinol, M. K.; Ceder, G.; Kresse, G.; Hafner, J. *Phys. Rev. B* **1998**, *58*, 2975.

(19) Reimers, J. N.; Dahn, J. R. *J. Electrochem. Soc.* **1992**, *139*, 2091.

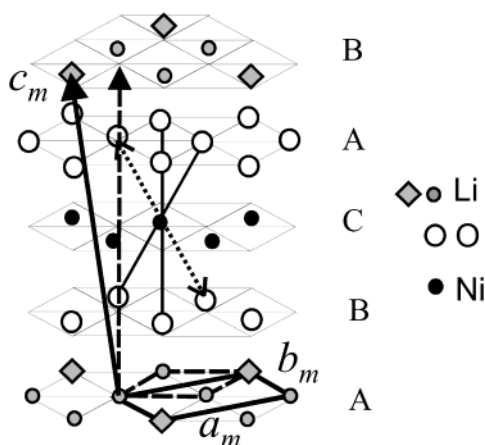


Figure 1. Schematic representation of the LiNiO_2 structure. Lithium ions in planes A and B are denoted with solid gray circles and diamonds. The diamonds are those Li ions that are at the extension of the Ni–O bond forming $180^\circ \text{Li}_\text{A}\text{–O–Ni}^{3+}\text{–O–Li}_\text{B}$ complexes. The cell with rhombohedral symmetry in the hexagonal setting is indicated by dashed lines. A hypothetical distortion of the Ni–O octahedra due to J–T effect is indicated by a dotted line, with the basic monoclinic cell indicated by bold lines.

$1.753)^{13}$ is larger than that in Li_xCoO_2 ($a_m/b_m = 1.733$).¹⁹ Moreover, the electrochemical data suggest that the mechanism for monoclinic distortion is not continuous across the whole domain $0.75 < x < 0.4$ and, throughout the literature on this material, two wide peaks can be observed in the derivative curve, $\text{d}x/\text{d}V$, in the monoclinic region.^{1,9,12,13,16} These peaks likely correspond to second-order phase transformations between ordered states. As pointed out by Ohzuku et al.,¹² multiple solid state reactions may actually occur in the monoclinic domain.

In this paper we resolve these conflicting arguments and, using first-principles calculations, demonstrate that Li-vacancy ordering and the Jahn–Teller activity of Ni^{3+} conspire and enforce each other to produce a monoclinic unit cell distortion. Such a synergetic effect of an electronic transition and ordering has to our knowledge not been documented before.

Methodology

Figure 1 shows a schematic representation of the LiNiO_2 structure and the relationship between the cells with rhombohedral and monoclinic symmetry. In a monoclinic cell a measure of the departure from the rhombohedral symmetry is given by the ratio between the a and b monoclinic lattice parameters, a_m/b_m . In an undistorted rhombohedral structure, this value would be $\sqrt{3}$. To study the evolution of the monoclinicity, a_m/b_m , with lithium content, x , we have calculated from first principles the lattice parameters and the total energy of a large set of Li_xNiO_2 ordered structures. First principles refers to the use of quantum mechanics to determine the structure or properties of materials at 0 K. In this particular work we use the *ab initio* pseudopotential method as implemented in the Vienna *Ab-initio* Simulation Package (VASP).^{20,21} This method

solves the Kohn–Sham equations within the local density (LDA) or the generalized gradient approximation (GGA) using ultra-soft pseudopotentials. In previous work,^{22,23} we found the use of GGA rather than LDA to be essential for correctly reproducing the Jahn–Teller distortion. Therefore, calculations were performed within the generalized gradient approximation. A plane wave basis set with a kinetic energy cutoff of 400 eV was used, which is adequate for these structures. The reciprocal space sampling was done in a $6 \times 6 \times 6$ k -point grid for structures containing two LiNiO_2 formula units, and in a $4 \times 4 \times 4$ or $2 \times 2 \times 2$ k -point grid for larger supercells. Relaxation was allowed and the final energies of the optimized geometries were recalculated so as to correct for changes in basis during relaxation.

The calculated energies and unit cell parameters of a large number of different Li-vacancy ordering structures were then used to obtain an approximation to the cell parameters and monoclinicity of the equilibrium (ordered and disordered) Li-vacancy arrangements in Li_xNiO_2 at room and higher temperatures. This is achieved by two distinct expansions to capture the effect of Li disorder respectively on the energy and monoclinicity. A *cluster expansion* is a mathematical tool to predict the properties of any arbitrary Li-vacancy configuration from the value of that property in a small set of well-ordered structures.¹⁸ When that property is the energy, the cluster expansion has the form of a generalized lattice Hamiltonian and can be used for example in conjunction with Monte Carlo simulations to predict the phase diagram and open circuit voltage as a function of composition at any temperature. More details of this approach can be found in refs 18 and 24. The cluster expansion for the energy of Li_xNiO_2 and its phase diagram will be presented in a separate paper.²⁴ Here, for the purpose of studying the monoclinicity we also cluster-expanded the a_m/b_m ratio. Such a cluster expansion relates the Li-vacancy distribution to the cell parameters. Hence, once the expansion is parametrized, it is possible to predict the cell parameters for any Li-vacancy arrangement in the Li_xNiO_2 system. The resulting cluster expansion contains 8 pairs and 4 triplets (see ref 24). The root-mean-square (rms) difference between the formation energies directly obtained from the first-principles calculation and the corresponding values as reproduced by the cluster expansion is approximately 6 meV. For the a_m/b_m cluster expansion a rms of 0.02 Å was obtained.

The cluster expansions of the energy and a_m/b_m ratio were then implemented in Monte Carlo simulations in the grand canonical ensemble. We used a periodic Monte Carlo cell containing a repeat unit of 5400 LiNiO_2 unit cells. At each temperature and chemical potential at least 2000 Monte Carlo passes per lattice sites were performed after which proper sampling (E or a_m/b_m) occurred over a minimum of 4000 Monte Carlo passes. The Monte Carlo simulation uses the energy expansion to equilibrate the Li-vacancy arrangement. For this arrangement the a_m/b_m ratio is calculated using the cluster expansion for the monoclinicity.

(22) Mishra, S. K.; Ceder, G. *Phys. Rev. B* **1999**, *59*, 6120.

(23) Arroyo y de Dompablo, M. E.; Marianetti, C.; Van der Ven, A.; Ceder, G. *Phys. Rev. B* **2001**, *63*, 144107.

(24) Arroyo y de Dompablo, M. E.; Van der Ven, A.; Ceder, G. *Phys. Rev. B* **2002**, *66*, 64112.

(20) Kresse, G.; Furthmüller, J. *Phys. Rev. B* **1993**, *48*, 13115.

(21) Kresse, G.; Furthmüller, J. *Comput. Mater. Sci.* **1996**, *6*, 15.

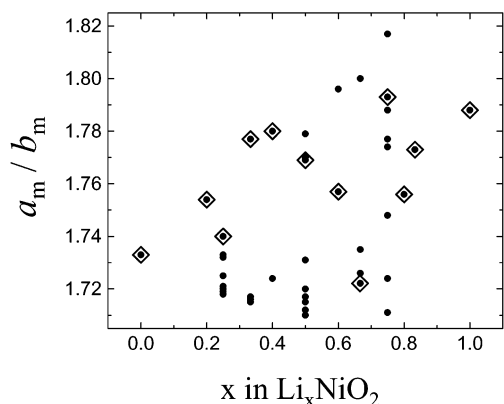


Figure 2. Monoclinicity calculated for ordered Li_xNiO_2 structures. Open diamonds correspond to the most stable structures at each composition.

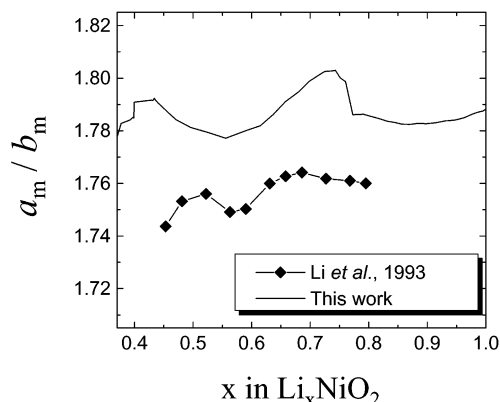


Figure 3. Calculated variation of a_m/b_m versus x in Li_xNiO_2 at room temperature. Experimental data taken from ref 13 are also plotted for comparison.

Evolution of the Monoclinicity in Li_xNiO_2 . Figure 2 shows the value of the a_m/b_m calculated for a set of 45 ordered Li_xNiO_2 structures. At most lithium compositions different Li-vacancy arrangements have been considered. The open diamonds correspond to the a_m/b_m value of the most stable structures at each composition. Several observations can be made: at a given composition, a wide range of monoclinicity is observed, indicating that Li-vacancy ordering has a strong influence on the extent of the monoclinic distortion. In the region where experimentally monoclinicity is observed ($0.4 < x < 0.75$), the monoclinicity varies considerably as the stable Li-vacancy ordering varies with composition. $\text{Li}_{0.75}\text{NiO}_2$ and $\text{Li}_{0.4}\text{NiO}_2$ present high monoclinic distortion, while $\text{Li}_{0.66}\text{NiO}_2$ is more stable when the structure is almost rhombohedral ($a_m/b_m = 1.72$).

However, Figure 2 represents the ground states at 0 K, and as T is increased, some partial (or complete) Li-vacancy disordering will occur. To obtain the monoclinicity under these conditions, Monte Carlo simulations were applied to obtain the state of Li-vacancy ordered as a function of the temperature and concentration. Using these equilibrated configurations as input to the cluster expansion for the a_m/b_m ratio results in the expected monoclinicity at room temperature. This result is shown in Figure 3. Experimental data taken from Li et al.¹³ are also plotted for comparison. The calculated a_m/b_m value slightly decreases in the range $1 < x < 0.8$. This decrease in monoclinicity is probably due to the fact that we have a much too large monoclinicity for

LiNiO_2 , whereas experimentally this is a rhombohedral compound. Then around $\text{Li}_{0.75}\text{NiO}_2$ there is a maximum, followed by a drop in the monoclinicity. A second maximum appears near $\text{Li}_{0.4}\text{NiO}_2$. In a separate study we found that $\text{Li}_{0.4}\text{NiO}_2$ is the most stable ordered phase in the Li_xNiO_2 phase diagram.²⁴ The occurrence of two maxima of monoclinicity indicates that the monoclinic region is rather complex and may actually consist of multiple phases. This would be consistent with the fact that two wide peaks appear in the experimentally measured differential capacity curve, $d\lambda/dV$.^{1,9,12,13,25}

The calculated data in Figure 3 are in qualitative agreement with the experimental data. However, some systematic shift in composition between the experimental and calculated monoclinicity maxima seems to be present. The calculated monoclinicity is also systematically higher. We believe that both these discrepancies, which prevent quantitative agreement, may be due to the fact that experiments are always performed on nonstoichiometric $\text{Li}_{1-z}\text{Ni}_{1+z}\text{O}_2$.^{14,26} In $\text{Li}_{1-z}\text{Ni}_{1+z}\text{O}_2$ the parameter z reflects the departure from stoichiometry that results from the presence of $2z$ Ni^{2+} ions in the material. Half of these Ni^{2+} ions are in the interslab space occupying lithium positions, and for charge compensation the other z Ni^{2+} ions are necessary in the NiO_2 layer. The value of z has a strong influence on the monoclinicity and the electrochemical properties.^{11,14,16,25} Actually, Bianchi et al. have proven that in materials with less Ni excess the monoclinic phase region extends toward higher depths of charge.²⁵ This may explain why different authors report a different lower limit for the monoclinic region: $x = 0.5$,¹³ $x = 0.45$,¹² $x = 0.4$,^{11,25,27} and $x = 0.38$.¹⁶ We expect the difference between stoichiometric and nonstoichiometric LiNiO_2 to be relevant through three mechanisms:

(1) The presence of Ni^{2+} in the interlayer space will reduce the magnitude of the monoclinicity. Whether the monoclinic distortion is originated by the Li-vacancy ordering or by a cooperative J–T distortion, Ni^{2+} in the interlayer space will perturb both. Indeed, it has been observed that for $z > 0.05$ the monoclinic distortion disappears and the deintercalation reaction proceeds in a rhombohedral host with no symmetry change.^{1,11,15,16} Also, substitution of Ni by other cations such as 20% Co has been shown to suppress the monoclinic distortion.¹

(2) A change in the effective Ni^{3+} concentration: If the driving force for the monoclinic distortion is the collective J–T distortion of Ni–O octahedra, a maximum in monoclinicity would occur at a critical Ni^{3+} concentration (y). In stoichiometry LiNiO_2 Ni^{3+} concentration (y) is related to the lithium content (x) as $y = x$. In $\text{Li}_{1-z}\text{Ni}_{1+z}\text{O}_2$ there are $2z$ Ni^{2+} ions, so $y = x - 2z$. Hence, the Ni excess would shift the maxima in monoclinicity to lower lithium compositions $\text{Li}_{x-2z}\text{Ni}_{1+z}\text{O}_2$.

(3) A change in the effective Li concentration: if the monoclinicity is caused by Li-vacancy ordering, the maximum in monoclinicity should be related to a critical lithium content (x). To reach the ordered Li_xNiO_2 in a

(25) Bianchi, V.; Bach, S.; Belhomme, C.; Farcy, J.; Pereira-Ramos, J.; Caurant, D.; Baffier, N.; Willmann, P. *Electrochim. Acta* **2001**, *46*, 999.

(26) Morales, J.; Perez-Vicente, C.; Tirado, J. L. *Mater. Res. Bull.* **1990**, *25*, 623.

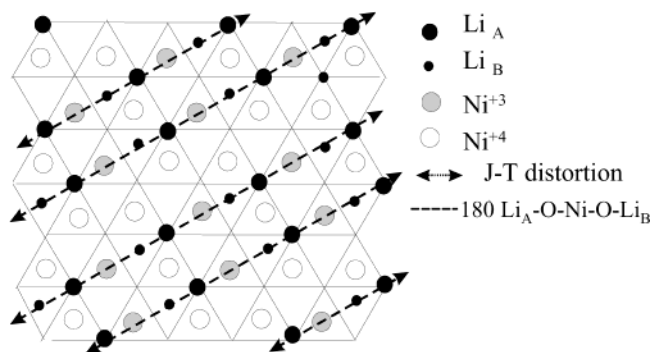


Figure 4. Representation of the cationic arrangement in $\text{Li}_{0.4}\text{NiO}_2$. Black circles represent planes of lithium ions (A and B). Gray and white circles denote respectively Ni^{3+} and Ni^{4+} ions. The $180^\circ \text{Li}_A\text{-O-Ni}^{3+}\text{-O-Li}_B$ configurations can clearly be seen.

stoichiometry sample, it is necessary to deintercalate $(1-x)$ lithium ions. But in $\text{Li}_{1-z}\text{Ni}_{1+z}\text{O}_2$ an amount of $(1-x)-z$ is required to reach $\text{Li}_x\text{Ni}_{1+z}\text{O}_2$. Hence, monoclinicity maxima due to Li-vacancy ordering will shift toward higher apparent Li concentration in experimental data.

These arguments may explain the shift between the experimental and calculated data (see Figure 3). The predicted maximum at $\text{Li}_{0.75}\text{NiO}_2$ shift toward lower lithium contents in the experimental data, consistently with a maximum due to J-T distortions. The calculated monoclinicity maximum at $\text{Li}_{0.4}\text{NiO}_2$ shifts to higher compositions in the experimental results, suggesting a Li-vacancy ordering driving force.

Origin of the Monoclinic Distortion: Coupling between Li-Vacancy Ordering and the Jahn-Teller Distortion

Figure 2 indicates that the monoclinicity depends strongly on Li-vacancy ordering. The qualitative correspondence between calculated and measured monoclinicity as a function of concentration (Figure 3) further supports this. The origin of the coupling between monoclinicity and Li-vacancy ordering lies in the weak Jahn-Teller activity of the Ni^{3+} ion. We have found that, in all ground states of the system, the monoclinic axis is also the axis of the local Jahn-Teller distortion around Ni^{3+} ions.²³ Furthermore, Li is always found to be present on the extensions of the $\text{Ni}^{3+}\text{-O}$ bond lengths along this axis. This generates $180^\circ \text{Li}_A\text{-O-Ni}^{3+}\text{-O-Li}_B$ pairs which in most structures form infinite chains. The Ni^{3+} ions in these lines of Li have a singly occupied and Jahn-Teller-distorted e_g orbital. Figure 4 illustrates this for the stable Li ordering in $\text{Li}_{0.4}\text{NiO}_2$: The J-T axis (its projection is shown with arrows in the figure) runs parallel to the $180^\circ \text{Li}_A\text{-O-Ni}^{3+}\text{-O-Li}_B$ configurations (dashed lines). We have found these stable $180^\circ \text{Li}_A\text{-O-Ni}^{3+}\text{-O-Li}_B$ in all ground states of the system.²³ We have previously explained the stability of these complexes as a coupling between the Li-vacancy ordering and the Jahn-Teller distortion of the Ni^{3+} ion: in undistorted Ni^{3+} the two e_g orbitals are degenerate and the intrinsic Jahn-Teller distortion only causes a small splitting,⁸ which in the real LiNiO_2 may not be strong enough to cause a collective Jahn-Teller distortion. When Li is present at the end of the $\text{Ni}^{3+}\text{-O}$ bond,

the hybridization with the Li 2s orbital lowers the energy of the octahedral e_g orbital so that its occupation becomes preferred over that of the other e_g orbital. This by itself does not create any $\text{Li}_A\text{-O-Ni-O-Li}_B$ interactions, but when the e_g orbital is J-T-active, the energy of the J-T distortion is maximal when the available charge is localized in completely filled or empty spin-orbitals (as opposed to partial occupation of all orbitals).²³ Hence, maximum J-T energy (and therefore distortion) is achieved when Li ions as much as possible hybridize with the *same* e_g^* orbital. This leads to effective $180^\circ \text{Li}_A\text{-Li}_B$ interaction connected by the filled e_g^* orbital of a Ni^{3+} ion. In the case when two of the 180° positions around a Ni ion are occupied with Li and the other four are empty, it can be expected that the d_{z^2} orbital is filled and oriented along the $\text{Li}_A\text{-O-M-O-Li}_B$ directions. The Ni ion would be in a mode of positive Jahn-Teller distortion (two long and four short bonds). In the case of four Li ions (two 180° pairs) around Ni, the $d_{x^2-y^2}$ orbital will hybridize with the Li 2s orbitals. Its filling will lead to a negative Jahn-Teller distortion (four long and two short bonds). The presence of six Li ions (all 180° pairs filled) will lower both e_g^* orbitals, but may still lead to a small Jahn-Teller distortion.

Using the mechanism described above, we can now explain the variation of monoclinicity with concentration in Li_xNiO_2 . The stable Li ordering at a given concentration will be determined by these Jahn-Teller-induced interplane Li-Li interactions as well as by the regular screened Coulombic interactions between Li ions. In the $\text{Li}_{0.75}\text{NiO}_2$ ground state 75% of all Ni ions are Ni^{3+} and 25% are Ni^{4+} .²⁴ In Figure 5 it can be observed that in this structure all Ni^{3+} ions are surrounded by either three or two $180^\circ \text{Li}_A\text{-O-Ni-O-Li}_B$ pairs, but never by a $180^\circ \text{Li-O-Ni-O-}$. Because their surroundings break the degeneracy between the e_g orbitals, these Ni^{3+} can undergo a strong Jahn-Teller distortion. The local J-T distortions (elongated $\text{Ni}^{3+}\text{-O}$ bonds) are aligned, resulting in a cooperative Jahn-Teller distortion. As a result, the material has substantial monoclinicity and the monoclinic axis is also the axis of the local Jahn-Teller distortion around Ni^{3+} ions. Notice that at 0 K (Figure 2) the monoclinicity of this structure is almost the same as the calculated distortion for LiNiO_2 . This seems reasonable given the Ni^{3+} configuration in $\text{Li}_{0.75}\text{NiO}_2$ (two Ni^{3+} with three 180° pairs and one Ni^{3+} with two 180° pairs). The unusual feature is that temperature increases the J-T distortion of the $\text{Li}_{0.75}\text{NiO}_2$ structure. We think this may be due to the fact that some Li disorder allows for arrangements with even stronger J-T distortion (such exist as can be seen in Figure 2). Though the $\text{Li}_{0.75}\text{NiO}_2$ structure in Figure 5 has the lowest energy at 0 K, its Li ordering is actually rhombohedral (only the Jahn-Teller distortion makes this material monoclinic³⁴) and it is not the arrangement that gives the largest monoclinicity. Hence, more monoclinic-like Li short-range order may actually increase the total monoclinicity at elevated temperature. When the Li content is reduced toward $x = 0.6$, the amount of Ni^{3+} decreases and the stable Li ordering at $x = 2/3$ is less amenable to Jahn-Teller distortion, as it is largely driven by Li-Li electrostatic interactions.²³ In the $\text{Li}_{2/3}\text{NiO}_2$ ground state one-third of the Ni ions are in

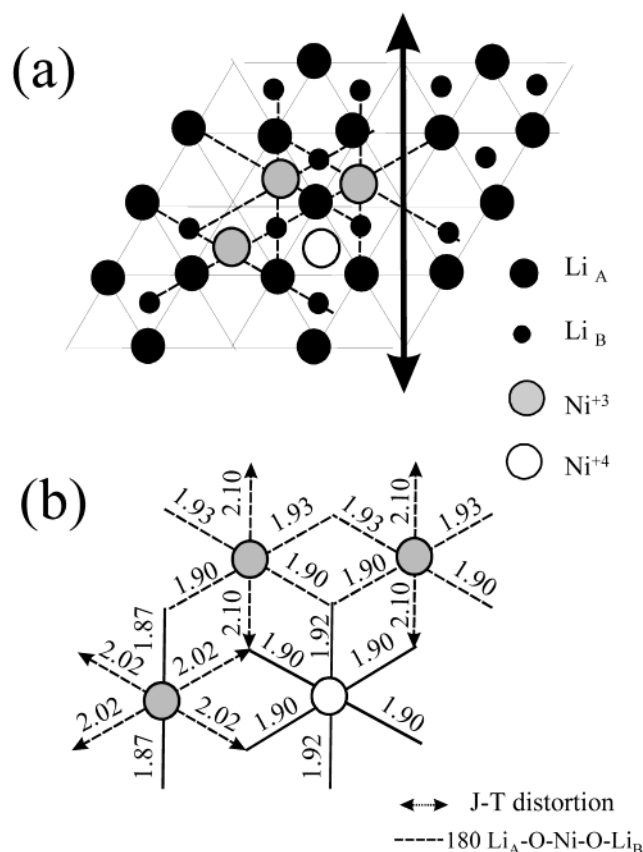


Figure 5. (a) Representation of the cationic arrangement in $\text{Li}_{0.75}\text{NiO}_2$. Black circles represent planes of lithium ions (A and B). Gray and white circles denote Ni^{3+} and Ni^{4+} ions in one unit cell, respectively. Dashed lines indicate the $180^\circ \text{Li}_A\text{-O-M-O-Li}_B$ configurations around Ni^{3+} ions and the bold arrow line the macroscopic monoclinic axis. (b) Schematic representation of Ni-O octahedra, showing the bonding distances. Local J-T distortions are indicated by arrows and $180^\circ \text{Li}_A\text{-O-M-O-Li}_B$ configurations around Ni^{3+} ions by dashed lines.

the trivalent state and two-thirds as $\text{Ni}^{3.5+}$. In this structure Ni^{3+} ions are surrounded by two 180° pairs, showing a small negative J-T distortion.²³ As x approaches 0.4, the monoclinicity increases again due to the very stable ordering at $x = 0.4$. As shown in Figure 4, the Li ordering in $\text{Li}_{0.4}\text{NiO}_2$ has only one $180^\circ \text{Li}_A\text{-O-Ni}^{3+}\text{-O-Li}_B$ pair around Ni^{3+} .

This model also explains the observations made by Peres et al.^{7,27} in the monoclinic region. Using EXAFS on delithiated $\text{Li}_{0.63}\text{Ni}_{1.02}\text{O}_2$,^{7,14} these authors found that at room temperature only a part of Ni^{3+} octahedral is

distorted. The authors conclude that if the distortion of all Ni-O octahedral in LiNiO_2 is not able to cooperatively distort the rhombohedral lattice, the distortion of only a few of them in $\text{Li}_{0.63}\text{Ni}_{1.02}\text{O}_2$ cannot induce the macroscopic distortion, claiming that the distortion is due to the Li-vacancy ordering.^{1,14,17,27} Considering Figure 3, it is now clear that the composition $\text{Li}_{0.63}\text{Ni}_{1.02}\text{O}_2$ is near the minimum in monoclinicity with the a_m/b_m being even lower than that in the starting compound LiNiO_2 . Therefore, it makes sense that no cooperative Jahn-Teller distortion could be found in $\text{Li}_{0.63}\text{Ni}_{1.02}\text{O}_2$.

Conclusion

We have calculated the evolution of the monoclinic distortion as a function of the lithium content in stoichiometric Li_xNiO_2 . In agreement with experimental results, maxima in a_m/b_m have been predicted to occur near $\text{Li}_{0.75}\text{NiO}_2$ and $\text{Li}_{0.4}\text{NiO}_2$. We find that the monoclinic distortion arises because of an unusual synergetic effect between the Li-vacancy ordering and the Jahn-Teller activity of Ni^{3+} . One may think of this phenomenon as a "Li-ordering induced Jahn-Teller distortion". The lack of Li-vacancy ordering possible in LiNiO_2 (as all Li sites are filled) therefore gives a weaker (in calculations) or nonexistent (in experiments) Jahn-Teller distortion. At $x = 0.4$ and $x = 0.75$ the stable Li orderings are particularly conducive to Jahn-Teller distortion, thereby creating two maxima in the monoclinicity.

Acknowledgment. This work was supported by the Department of Energy under Grant DE-FG02-96ER 45571. We express our sincere gratitude to Prof. C. Delmas for helpful discussion on this work. Discussions with C. Marianetti and Dr. A. Van der Ven were also helpful in developing the ideas in this paper. G.C. acknowledges support from Union Minière in the form of a Faculty Development Chair. Computing resources from NPACI, the National Partnership for Advanced Computing Infrastructure (NSF), are gratefully acknowledged. Support from the Singapore MIT Alliance is gratefully acknowledged. M.E.A.D. is thankful for support from Ministerio de Educacion Cultura y Deportes (Spain) and from Universidad Complutense de Madrid (Spain).

CM020239+

(27) Peres, J. P. Doctoral Thesis, L'Universitè Bourdeaux I, Nov 1996.